11th International Conference on Vibration Problems
Z. Dimitrovová *et al.* (eds.)
Lisbon, Portugal, 9-12 September 2013

THE DEVELOPMENT AND MITIGATION OF GROUND MACH CONES FOR HIGH SPEED RAILWAYS

Peter K. Woodward*, Omar Laghrouche, Abdellah El-Kacimi

Infrastructure & Environment Scotland, Heriot-Watt University, Edinburgh, EH14 4AS, UK
{P.K.Woodward, O.Lagrouche, A.Elkacimi}@hw.ac.uk

Keywords: Ground Mach Cones, Track Critical Velocity, Rayleigh Waves, High-speed

Abstract. *In this paper the application of the DART3D (Dynamic Analysis of Railway Track – 3D) finite element program is used to model the development of ground Mach Cones for high-speed trains approaching the ground Rayleigh wave velocity, particularly for both weak and weak-medium stiff subgrades. Multiple train axles and complete train-track interaction are included in the studies. The results show, in a systematic way, how the Mach Cone is formed as the train speed increases incrementally. The geometrical angle of the Mach Cone is compared to analytical solutions and good agreement found. The difference between the Rayleigh wave velocity and the track resonant velocity is further highlighted through parametric studies and through 3-dimensional graphical representations of the advancing wave front. The effect of the Mach Cone development on the transient response of a sleeper is also shown, as is the development of non-linearity in the stress strain response and the subsequent effect on the track deflections.*

1 INTRODUCTION

As train speeds approach critical values rapid deterioration of the track, ballast and sub-ballast can occur due to Rayleigh wave and track critical velocity effects [1, 2]. Very soft soils may have a Rayleigh wave speed of only 30-40 m/s [3, 4]. Railway track systems built on soft ground, perhaps on shallow embankments, can develop critical speeds lower than 200 km/h [3, 5-9].

The operational speed of the planned UK High Speed 2 line is 360 km/h, but it will be designed for 400 km/h. It is therefore essential to develop a clear understanding of the mechanisms of dynamic track response and the methods to reduce ground vibration. Such methods may include CMC columns, vibro concrete columns and stone columns. As critical values are approached the dynamic train response becomes very complicated due to the coupled nature of the train-track interaction [10, 11] and the ground dynamics. In the general literature the large deflections at the Ledsgard site in Sweden, due to critical velocity effects, has been documented [2, 3, 6, 12-13]. However data on other sites is very limited due to the significant track deflections generated when trains try to run at these critical speeds [5]. The Ledsgard site is however complicated in that multiple track layers are present, each with their own Rayleigh wave velocity, and the presence of an embankment. In this paper finite element analyses are performed using a purposely written finite element program in an attempt to help analyse the different mechanisms contributing to the track response. Both linear and non-linear analyses are performed; in the latter case a stone column problem is considered as a form of track mitigation.

2 FINITE ELEMENT PROGRAM DART3D

The numerical program is based on 3-dimensional finite elements and is called DART3D (Dynamic Analysis of Railway Track 3D). Although the program has been used for a few years to look at track geo-dynamics [9], including the development of Mach Cones [10, 11] it is continuously being developed.

The analysis is fully coupled, i.e. the train suspension system is coupled to the vertical deflection of the track. This means that the train and track can interaction with each other, even when the soil response is non-linear. The program uses a time domain approach to model these non-linear effects and energy absorbing boundaries are implemented to prevent stress-wave reflection.

2.1 Train model

For the quarter train model used in this paper the equations representing the system components [11, 14, 15] are,

$$\begin{pmatrix} k_c & -k_c & 0 \\ -k_c & k_b+k_c & -k_b \\ 0 & -k_b & k_b \end{pmatrix}\begin{pmatrix} w_c \\ w_b \\ w_w \end{pmatrix}+\begin{pmatrix} c_c & -c_c & 0 \\ -c_c & c_b+c_c & -c_b \\ 0 & -c_b & c_b \end{pmatrix}\begin{pmatrix} \dot{w}_c \\ \dot{w}_b \\ \dot{w}_w \end{pmatrix}+\begin{pmatrix} \overline{m}_c & 0 & 0 \\ 0 & \overline{m}_b & 0 \\ 0 & 0 & m_w \end{pmatrix}\begin{pmatrix} \ddot{w}_c \\ \ddot{w}_b \\ \ddot{w}_w \end{pmatrix}=\begin{pmatrix} \overline{m}_c g \\ \overline{m}_b g \\ m_w g + F_{wr} \end{pmatrix} \quad (1)$$

Where w_c, w_b and w_w are the vertical displacements of the car body, bogie and wheel, m_w is the wheel mass, $\overline{m}_c$ and $\overline{m}_b$ are representations of the car body and bogie masses ($\overline{m}_c = m_c/8$ and $\overline{m}_b = m_b/4$). k_b and k_c are the primary and secondary suspension stiffness and c_b and c_c

the corresponding damping coefficients. The train suspension system modelled in this paper is similar to the Thalys high-speed train [16].

The train properties assumed for both the linear and non-linear analysis are shown in Table 1 below.

Suspension Property	
Axle Load (kN)	181
Primary Suspension	
Stiffness (MN/m)	3.28
Damping (kNs/m)	90
Secondary Suspension	
Stiffness (MN/m)	1.31
Damping (kNs/m)	30

Table 1: Train suspension parameters used in analysis

2.2 Track model

Although DART3D is continuously being developed, the current version is able simulate the track structure, including the rails, sleepers, pad, ballast and subgrade layers. The 3D aspect of the program can generate long computational times as it uses an explicit time integration scheme (typically $\Delta t=8 \times 10^{-6}$ s). Full details about the finite element program can be found in [8, 11].

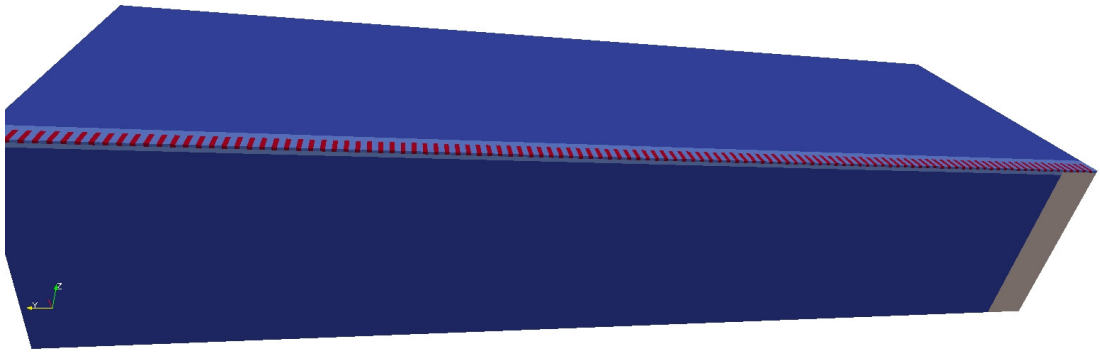

Figure 1: Mesh used in ground dynamics simulation

Figure 1 shows the mesh used in the current studies and Table 2 shows the material parameters assumed in the linear studies. In total 42,450 20-noded brick elements are used in the analysis for the sub-structure and 424 beam-column elements for the rail (the rail is omitted for clarity in Figure 1). The ballast is assumed to be 300 mm deep below the sleeper bottom and extends a distance of 1400 mm from the track centre line. The boundaries are fixed on the base and energy absorbing dashpots on the sides.

Ballast	
Young's Modulus (MPa)	124
Poisson's Ratio	0.4
Rayleigh Damping (%)	5
Density (kg/m^3)	1800
Clay Subgrade	
Young's Modulus (MPa)	24.5
Poisson's Ratio	0.45
Rayleigh Damping (%)	5
Density (kg/m^3)	1500

Table 2: Ballast/soil parameters used in linear analysis

The linear subgrade has a Rayleigh wave speed of approximately 70 m/s. The track resonant velocity for the particular train used is only slightly higher than this.

2.3 Damping

Rayleigh damping is used in the analysis with frequencies of ω_1=32 rad/s and ω_2=34 rad/s. The Rayleigh damping coefficients α and β can be found from:

$$\alpha = \frac{2\omega_1\omega_2\xi}{100(\omega_1 + \omega_2)} \tag{2}$$

and

$$\beta = \frac{2\xi}{100(\omega_1 + \omega_2)} \tag{3}$$

Where ξ is the target damping ratio and is set at 5%. In the linear analysis the damping ratio remains constant throughout the analysis, however in the non-linear case the damping ratio changes with the induced shear strain.

2.4 Linear analysis

Often numerical models of track response for train speeds leading up to the Rayleigh wave velocity and the track resonant velocity use linear models; this is primarily due to the long computational times required. The stiffness and damping properties of the geo-materials are then modified depending on the predicted induced shear strain in the subgrade, which is a function of train speed and percentage of Rayleigh and track resonant velocity. Calculation of the track critical velocity for a beam on an elastic foundation was given by [5]. Moving load simulations can also be found from [17, 18].

In the following example the subgrade stiffness is however kept constant in order to illustrate the different developing mechanisms (i.e. not to confuse the issue of changing stiffness and dynamics with the developing wave fronts). The effect of reducing the ballast and subgrade stiffness would of course be to increase the track deflection and reduce the ground wave speeds. This type of analysis is considered in Section 3 where a non-linear model is used to study track behaviour including stone column implementation.

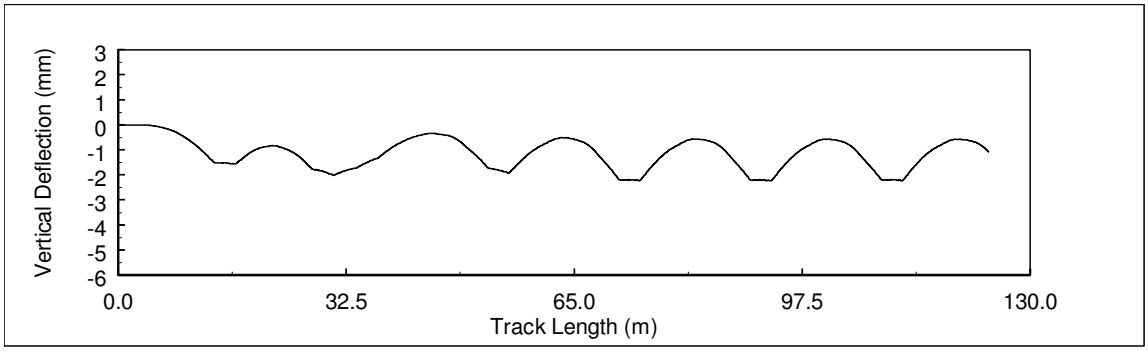

(a) Speed=47 m/s

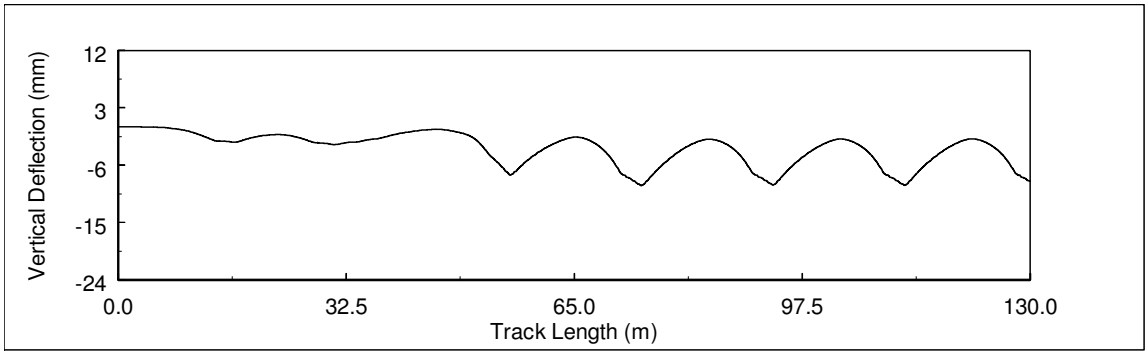

(b) Speed=62 m/s

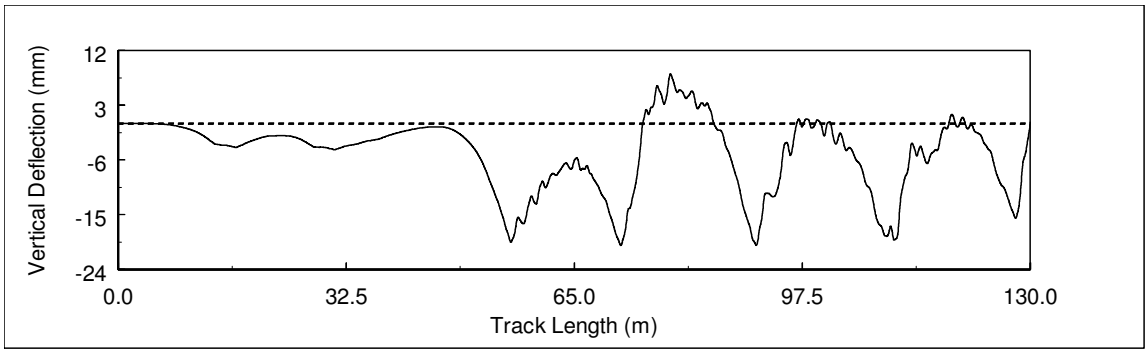

(c) Speed=75 m/s

Figure 2: Transient vertical deflection of a typical sleeper with train speed using the 3D model

The response of a typical sleeper at a train speed of 47 m/s is shown in Figure 2a. The response is highly regular with all bogies having an individual imprint. The peak transient vertical deflection is approximately 2 mm. Figure 2b shows the track response at a train speed of 62 m/s (note the change in scale when compared to Figure 2a). The train speed has now passed 70% of the subgrade Rayleigh wave speed of the subgrade where dynamic effects are known to develop rapidly. It should be remembered that the high degree of track deflection would induce a greater degree of non-linearity and damping, however as discussed previously, the properties in this example are kept constant to illustrate the different developing conditions. The transient deflection is around 6.5 mm and a ground Mach Cone is developing. In Figure 2c a ground Mach Cone has developed and the track resonant velocity has been

achieved leading to large deflections, including track uplift. The shape and magnitude of these deflections would also be highly dependent on the train axle spacing and material damping.

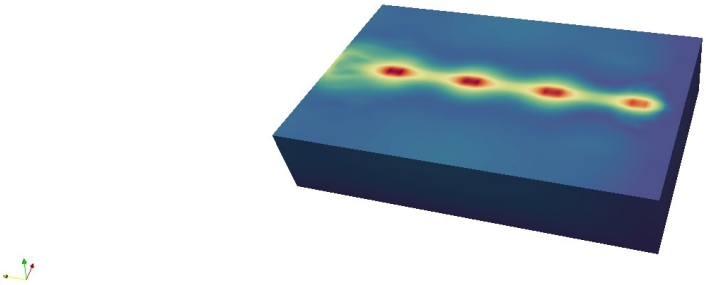

(a) Speed=47 m/s

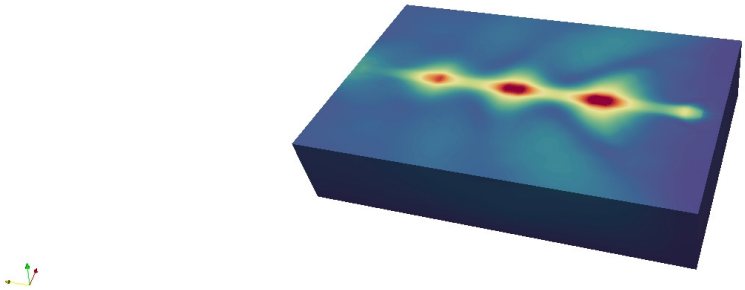

(b) Speed=62 m/s

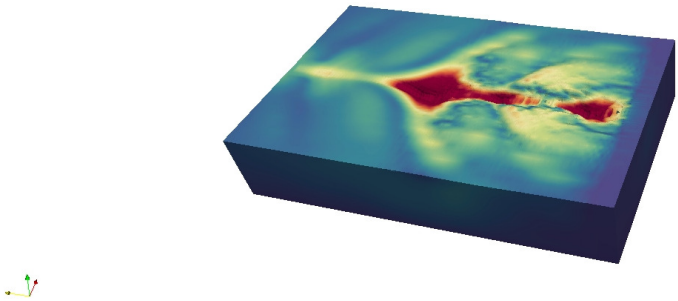

(c) Speed=75 ms

Figure 3: Development of the ground Mach Cone and track dynamics at various train speeds

The development of the ground Mach Cone as the train speed increases towards the Rayleigh ground wave and track resonant velocity is clearly shown in Figure 3. Figure 3a shows that when the speed of the train is 47 m/s the ground pattern is symmetrical with little ground wave transmission. At 62 m/s the developing Mach Cone can be seen, which is indicated by the track deflections shown in Figure 2b. When the train speed passes the subgrade Rayleigh wave velocity and reaches the track resonant velocity (which in this particular case is only

slightly higher) the development of a full Mach Cone and track uplift is observed. The depth of the cone can be clearly seen in Figure 4 which shows a cut-away section through the track centre line (i.e. a cut-away of Figure 3c).

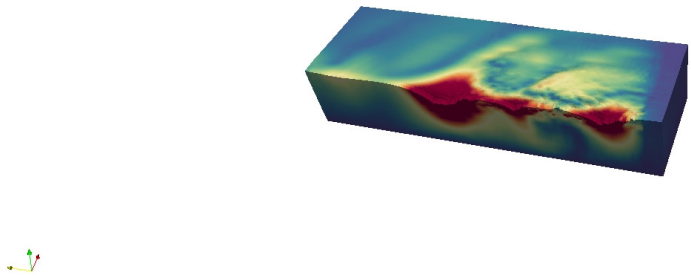

Figure 4: Cut-away showing the ground dynamics at track resonant velocity (low damping)

Conventional Mach Cone theory indicates that the angle of the wave front can be given by the following equation

$$\alpha = \sin^{-1}\left(\frac{1}{\frac{V_T}{V_R}}\right) \tag{4}$$

Where V_T is the train speed and V_R is the Rayleigh wave velocity and α is half the wave-front angle (the total angle is therefore 2α). For Figure 3c, $\alpha \approx 120^o$. As the train speed exceeds the subgrade Rayleigh wave velocity the angle becomes more acute. For low ballast depths the Rayleigh wave velocity and the *track critical velocity* (based on a beam on an elastic foundation analysis [5]) would be similar. For embankments and/or upper track stiffness increases, the combined Rayleigh velocity would be higher than the *in-situ* subgrade only Rayleigh wave velocity due to the stiffening effect. In this way the track Rayleigh wave dynamic characteristics can be improved; however careful analysis of the track resonant condition still needs to be made.

The prediction of both of these parameters is essential when examining track mitigation strategies and hence allow for higher line speeds. This is especially important when analysing complex 3D geometric shapes, reinforcement strategies and non-linear effects as these all modify the Rayleigh wave velocity and train-track resonant velocity. The use of 3D finite elements therefore becomes a very useful tool for track prediction at high-speed.

3 NON-LINEAR MODELLING

In this paper the stiffness of the non-linear geo-materials is modelled using the Universal model which was developed by [19].

3.1 Non-linear stiffness

In the non-linear model the resilient modulus of the soil is related to the mean and deviatoric stress though:

$$E_r = k_1 p_{atm} \left(\frac{3p}{p_{atm}} \right)^{k_2} \left(1 + \frac{q}{p_{atm}} \right)^{k_3} \tag{5}$$

where, p_{atm} is atmospheric pressure; p and q are mean and deviatoric stresses respectively; k_1, k_2 and k_3 are the material parameters. Assigning a negative or positive value to k_3 can model the softening or hardening effect of the shear stress on the resilient modulus. The material parameters used in this paper are presented in Table 3.

Ballast	
k_1	1400
k_2	0.2
k_3	-1.35
Poisson's Ratio	0.4
Density (kg/m^3)	1800
Clay Subgrade	
k_1	245
k_2	0.
k_3	-0.4
Poisson's Ratio	0.45
Density (kg/m^3	1500

Table 3. Ballast and clay material parameters used in non-linear analysis

3.2 Non-linear damping

The non-linear damping is based on [20]:

$$\xi = d_1 + \left(d_2 \left(1 + 0.15 \left(100 \gamma^{dev} \right)^{-0.9} \right)^{0.75} \right) \tag{6}$$

Where ξ is the damping ratio, γ^{dev} is the deviatoric shear strain and d_1 & d_2 are material parameters. The parameters used in this paper are shown in Table 4.

Ballast	
d_1	1.5
d_2	15
Clay Subgrade	
d_1	3
d_2	12

Table 4. Track damping material parameters used in non-linear speed effect analysis

Figure 5 shows an analysis using the non-linear model for a train speed of 75 m/s and assuming that small diameter stone columns exist below the ballast layer. Using the parameters in Tables 3 and 4 the analysis predicts a very high downward deflection due to a high degree of non-linearity and subsequent uplift (i.e. although columns have been added the high-degree of non-linearity still predicts track resonant velocity). Full calibration of the model would of course be required at a real site and work to simulate Ledsgard using the non-linear model is currently underway. To the Authors' knowledge, Ledsgard represents the only site where data of this kind is available in the international literature.

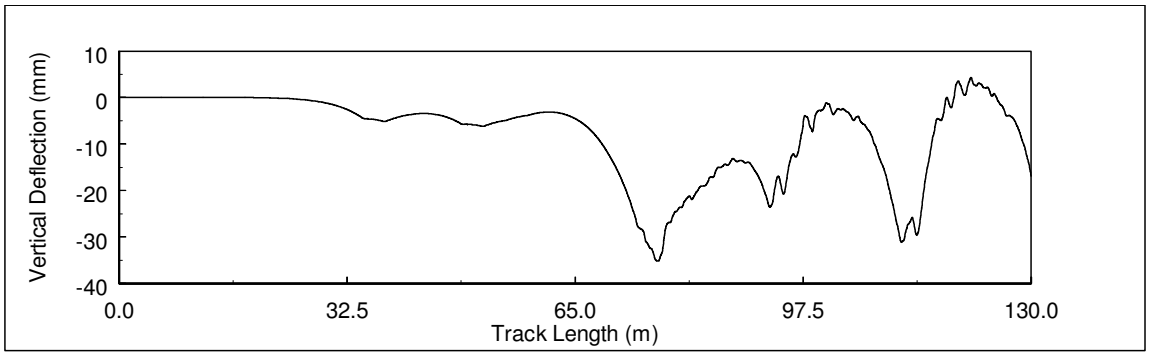

Figure 5: Effect of non-linearity on the track response at train speed=75 m/s

4 CONCLUSIONS

- A numerical model capable of modelling high-speed track dynamics has been proposed.
- The development of the ground Mach Cone at Rayleigh ground wave velocity and subsequent train-track resonant velocity leads to high track deflections.
- At the track resonant velocity track uplift is predicted.
- A high degree of non-linearity is developed as the Rayleigh and track resonant velocity is achieved, this has a significant impact on the track behaviour.

ACKNOWLEDGEMENTS

The work was performed with support from the Engineering and Physical Sciences Research Council under grant EP/H027262/1. Their support is hereby gratefully acknowledged.

REFERENCES

[1] Adolfsson, K., Andreasson, B., Benktsson, P.E. and Zakrisson, P. High speed train X2000 on soft organic clay-measurements in Sweden. 12th European Conf. of Soil Mech. and Geot. Eng. 1999. Amsterdam.

[2] Madshus C and Kaynia A. High speed railway lines on soft ground, dynamic behaviour at critical speed. J Sound Vib 2000; 231: 689–701.

[3] Madshus, C., Lacasse, S., Kaynia, A. And Harvik, L. (2004) Geodynamic challenges in high speed railways projects. ASCE Proc Geotechnical Engineering for Transportation Projects (GSP 126)

[4] Woldringh, R.F. and New, B.M, "Embankment design for high speed trains on soft soils". Geotechnical Engineering for Transportation Infrastructure, Barends et al (eds), Balkema, Rotterdam, 1999.

[5] Krylov, V.. On the theory of railway-induced ground vibration. Journal de Physique IV, 4 (C5): 769–772, 1994.

[6] Takemiya, H. Simulation of track-ground vibrations due to a high-speed train: the case of X-2000 at Ledsgard. Journal Sound and Vibration 261, 2003, 503-526.

[7] Lombaert G, Degrande G, Kogut J and Francois S. The experimental validation of a numerical model for the prediction of railway induced vibrations. J Sound Vib 2006; 297: 512–535.

[8] Banimahd, M. (2008) Advanced finite element modelling of coupled train-track systems: a geotechnical perspective. Thesis for the Degree of Doctor of Philosophy, Heriot-Watt University, UK.

[9] Banimahd, M., Woodward, P.K., Kennedy, J. and Medero, G.M. Three dimensional modelling of high-speed ballast railway tracks. Proceedings of the Institution of Civil Engineers, Transport Journal, 166 April 2013 Issue TR2, Pages 113–123 http://dx.doi.org/10.1680/tran.9.00048, 2012

[10] El-Kacimi, A., Woodward, P.K., Laghrouche, O. And Medero, G. (2011). 3D finite element modelling of ground dynamics for high speed trains. Proc. 11th International Railway Engineering Conference, University of Westminster, London.

[11] El-Kacimi, A., Woodward, P.K., Laghrouche, O. And Medero, G. Time Domain 3D Finite Element Modelling of Train-induced Vibration at High Speed. Internal Journal of Computers & Structures, Vol 118, 66-73, doi.org/10.1016/j.compstruc.2012.07.011, 2013.

[12] Hall, L. (2000). Simulations and analyses of train-induced ground vibrations, a comparative study of two and three-dimensional calculations with actual measurements, PhD Thesis, Royal Institute of Technology, Sweden.

[13] Paolucci, R. Maffeis, A. Scandella, L., Stupazzini, M. and Vanini, M. Numerical prediction of low-frequency ground vibrations induced by high-speed trains at Ledsgard, Sweden. Soil Dynamics and Earthquake Engineering 23, 2003, 425-433.

[14] Lei, X., and Noda, N.A. 2002. Analyses of dynamic response of vehicle and track coupling system with random irregularity of track vertical profile. Journal of Sound and Vibration, 258, 147–165.

[15] Lei, X., and Mao, L. 2003. Dynamic response analyses of vehicle and track coupled system on track transition of conventional high speed railway. Journal of Sound and Vibration, 271, 1133-1146.

[16] Degrande, G. and Schillemans, L. Free field vibrations during the passage of a Thalys high-speed train at variable speed. Journal of Sound and Vibration, 247(1), 131-144, 2001.

[17] Dietermann H and Metrikine A. The equivalent stiffness of a half-space interacting with a beam. Critical velocities of a load moving along a beam. Eur J Mech A: Solids 1996; 15: 67–90.

[18] Yang, Y.B., Hung, H.H. and Chang, D.W., "Train-induced wave propagation in layered soils using finite/infinite element simulation". Soil Dynamics Earthquake Engineering, 23: 263-278, 2003.

[19] Uzan, J., Resilient characterization of pavement materials 1992. International Journal for Numerical and Analytical Methods in Geomechanics, 16(6): 453-459.

[20] Rollins, K.M., Evans, M.D., Diehl, N.B. and Daily, W.D. Shear modulus and damping relationships for gravels, Journal of Geotechnical and Geoenvironmental Engineering, Vol 124, No. 5, 396-405, 1998. http://dx.doi.org/10.1061/(ASCE)1090-0241(1998)124:5(396)).